

Behavior of FRP strengthened RC brick in-filled frames subjected to cyclic loading

Balvir Singh^{1a}, R. Siva Chidambaram^{2b}, Shruti Sharma^{*1} and Naveen Kwatra^{1c}

¹Department of Civil Engineering, Thapar University, Patiala, Punjab, India

²CSIR-Central Building Research Institute, Uttarakhand, Roorkee-247667, India

(Received April 24, 2017, Revised July 11, 2017, Accepted July 13, 2017)

Abstract. Fiber reinforced polymer (FRP) sheets are the most efficient structural materials in terms of strength to weight ratio and its application in strengthening and retrofitting of a structure or structural elements are inevitable. The performance enhancement of structural elements without increasing the cross sectional area and flexible nature are the major advantages of FRP in retrofitting/strengthening work. This research article presents a detailed study on the inelastic response of conventional and retrofitted Reinforced Concrete (RC) frames using Carbon Fibre Reinforced Polymers (CFRP) and Glass Fiber Reinforced Polymers (GFRP) subjected to quasi-static loading. The hysteretic behaviour, stiffness degradation, energy dissipation and damage index are the parameters employed to analyse the efficacy of FRP strengthening of brick in-filled RC frames. Repair and retrofitting of brick infilled RC frame shows an improved load carrying and damage tolerance capacity than control frame.

Keywords: retrofitting; vibration; brick infills; RC frame; frequency response function; damage index; GFRP; CFRP; vibration monitoring

1. Introduction

North India is more vulnerable to earthquakes; especially the Himalayan belt is very active earthquake prone zone. The past earthquakes in India exposed the inadequacy of existing in-filled framed RC structures to earthquakes and the observed damages in the buildings and other structures during the earthquakes requires a need to explore possible new techniques for repair, retrofitting and strengthening of these structures. The inadequate reinforcement detailing, lack of confinement in the joint region and absence of proper anchorage in column leads to collapse of beam-column joints during an earthquake. In most of the cases, beam-column joint and soft-storey failure significantly affects the global behavior of the RC frames. The masonry infill in RC structure is anisotropic material having wide range of deformation, strength and energy dissipation properties. The lateral displacement during a strong ground motion causes severe damage to infill and to the frame. A proper retrofitting or strengthening technique is required to strengthen the existing in-filled RC framed structure or to retrofit the impaired structure to provide a sufficient protection. Up-gradation of existing structure to meet the current codal recommendations or to satisfy the

current requirements and seismic strengthening of existing structure to meet the earthquake resistant measures in critical zones requires advanced techniques rather than traditional methods.

There is no standard outlined procedure for retrofitting and strengthening of existing structures in India. Few countries such as America, Japan, New Zealand, have special guidelines in this respect. Understanding the behavior of retrofitted structure is essential but still insufficient. The conventional methods of seismic retrofitting, generally adopts construction of shear wall, providing steel bracing, increasing the dimensions of existing members using steel/concrete jacketing etc. The dimensional increment increases the dead load and changes the stiffness behavior of the structural member. On the other hand, many advanced materials such as Fiber Reinforced Polymers (FRP), Shape Memory Alloys (SMA) etc. are available as an alternate source to the conventional materials and techniques in upgrading a structure. Based on the configuration of building, different methods and techniques of retrofitting are available and also it is not mandatory to choose only one particular strengthening scheme for a structure.

In retrofitting of large structure, cost- minimization of materials with maximization of seismic resistant measures is necessary. Advanced strengthening techniques require lesser labor and its immediate response to the need leads us to choose them instead of conventional techniques. External Fiber Reinforced Polymer (FRP) wrapping is one of the prime techniques in strengthening of an existing structure because of its various advantages such as lesser weight, higher strength and flexibility to use in all kinds of structural elements, easy workmanship etc. Mukherjee and Joshi (2005) observed that the retrofitted connections using

*Corresponding author, Associate Professor

E-mail: shruti.sharma@thapar.edu

^aPh.D. Student

E-mail: sandhu_balvir@yahoo.co.in

^bLecturer

E-mail: krsinelastic@gmail.com

^cProfessor

E-mail: nkwatra@thapar.edu

FRP sheets prevent its brittle shear failure and also significantly improved their displacement ductility and energy dissipation capacity. The use of GFRP and CFRP as external wrapping has been found as an effective method for upgrading deficient RC beams, columns and beam-column joints (Said 2009, Ceroni 2010, Lakshmikantham *et al.* 2012, Shraideh and Aboutaha 2013, Hou *et al.* 2015, Yurdakul and Avsar 2015, Kakaletsis 2016, Tunaboyu and Avşar 2017). The researchers have reported in general, an increase in the load carrying capacities, improvement in flexural and shear capacities and enhancement in ductility of the structural elements due to confining effects of FRP wraps. The behavior of CFRP strengthened beam under monotonic load confirmed the applicability of cyclic loading method to evolve the stiffness degradation and damage assessment and it was reported that the bonding between the CFRP wrap and the concrete governs the strength of the repaired beams which outperformed the undamaged control beam (Lakshmikantham *et al.* 2013). Significant increase in the strength and ductility of concrete can be achieved by CFRP composite jackets and the confinement modulus and the confinement strength of the composite jacket has been identified as the two critical parameters in describing the system confinement effectiveness (Omar and Stefan 2014). Structural repairing of damaged reinforced concrete beam-column assemblies with CFRPs was undertaken and it was observed that capacities of the damaged members were mostly recovered by the application of CFRP (Yurdakul and Avsar 2015). The effectiveness of the use of modern repair schemes for the seismic retrofit of existing RC structures were assessed on a comparative experimental study of carbon fiber-reinforced polymer (CFRP) strips and sheets for the repair of reinforced concrete members of RC frames, damaged because of cyclic loading and it was observed that the repaired frames recovered their strength, stiffness and energy dissipated reasonably and CFRP sheets were more effective than CFRP strips due to the proper anchorage (Kakaletsis 2016). The effectiveness of the seismic repair scheme for the damaged captive-columns with CFRPs was investigated in terms of response quantities such as strength, ductility, dissipated energy and stiffness degradation and it was observed that the overall response of the bare frame was dominated by flexural cracks whereas brittle type of shear failure in the column top ends was observed in the specimens with partial infill walls. Capacity of damaged members was recovered by the repair scheme and ultimate displacement capacity of the damaged frame was improved considerably by CFRP wrapping (Tunaboyu and Avşar 2017). Hence, the GFRP and CFRP wraps have proved to be efficient repair and strengthening options for RC structural members. However the response of retrofitted and strengthened RC structures by application of FRP's needs to be monitored regularly as the cracks are covered by external strengthening layers.

Several researchers have relied on the use of vibration measurements for system identification and damage detection. Damage monitoring for structures using change in the dynamic properties such as natural frequency, mode shape and frequency response function (FRF) has been

suggested by various researchers and can be effectively used for damage detection. It is generally assessed by calculating the Damage Index (DI). This index depends upon specific damage parameters such as structural stiffness, strength deterioration, stiffness degradation, deformation, energy dissipation and dynamic properties of structure. Different scientists developed different damage indexes depending upon specific damage parameters. The well known combined damage index method was proposed by Park and Ang (1985). This index is calculated as a linear combination of maximum displacement response and total hysteretic energy dissipation under cyclic load. Wang *et al.* (2005) investigated the coupled bending and torsional vibration of a fiber-reinforced composite cantilever beam with an edge surface crack and reported that the natural frequency shifts, along with observations on the mode shape changes due to surface crack and hence, can be used to detect both the crack location and its depth for on-line Structural Health Monitoring (SHM). Ahmed *et al.* (2009) revealed that Vibration Based Damage Identification (VBDI) applied to structural health monitoring can be very useful in interpreting the global vibration response of a structure to identify local changes (e.g., damages) in it. But due to complicated features of real life structures there are some uncertainties involved in its key input parameters (e.g., measured frequencies and mode shape data) whereas output is highly sensitive to errors in modal parameters. The authors suggested that if vibration based methods are to be used for identification of damages they should be incorporated with semi analytical methods such as neural networks and statistical pattern recognition techniques for better accuracy which can result in structural health assessment. Ooijevaar *et al.* (2010) applied VBDI method for experimentally investigating the dynamic response of an intact and a locally delaminated 16-layer unidirectional carbon fibre reinforced *T*-beam. A force-vibration set-up including a laser vibrometer system was employed to measure the dynamic behaviour of the *T*-beam. The Modal Strain Energy Damage Index algorithm was applied using the bending and torsion modes. Kanwar *et al.* (2010) used and reported the effectiveness of vibration based parameters and measurements for health monitoring of RC buildings. Vimuttasongviriya *et al.* (2011) used VBDI to study the effect of lateral load on the damage indexes of RC frame strengthened using GFRP sheets. The author reported that the use of GFRP for structural retrofitting increased the lateral load capacity and ductility of the RC frame significantly. Further, the damage indexes of retrofitted frame reduce indicating better performance as compared to control frame. Xu *et al.* (2012) investigated different framed structures with different joint damage scenarios introduced by loosening the bolts connecting the beams and columns by using direct displacement measurement under base excitations. It was reported that the proposed time domain methodology could easily identify the variation of inter storey stiffness due to the joint damage with acceptable accuracy without any modal shapes and frequencies extracted from a dynamic test. The proposed approach provides an alternative way for damage detection of engineering structures by the direct use of

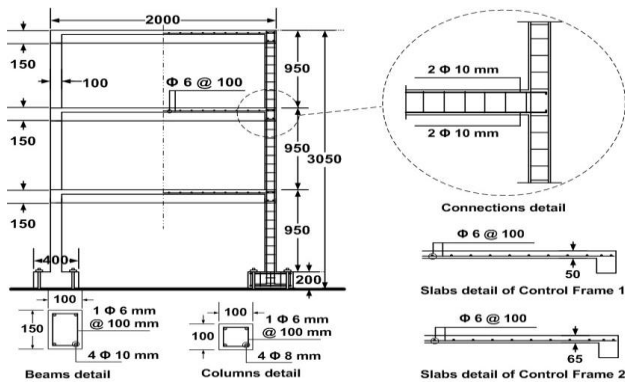


Fig. 1 Reinforcement details of RC frame

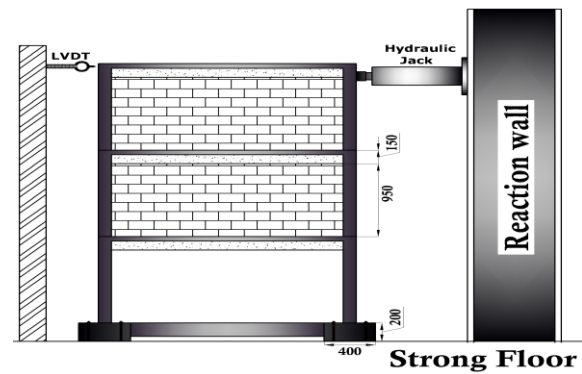


Fig. 2 Schematic diagram of RC frame test set-up

structural dynamic displacement measurements. Kanwar *et al.* (2016) studied dynamic characteristics of different RC buildings under different levels of damage using VBDI approach and it was used to develop a correlation between damage in the RC buildings with its known dynamic characteristics using artificial neural network models. However, this use of damage index has not been preferred to monitor damage in retrofitted structures in proper way because the cracks are covered by strengthening material layers. Also the VBDI approach has not been used to monitoring response due to damages in brick in-filled RC framed structures repaired with composites.

This research work mainly focuses on the investigation of the inelastic behavior of a seismically damaged brick infilled RC frame retrofitted with GFRP and CFRP wraps along with monitoring of the same using VBDI. A three-storey brick infilled RC frame structure was constructed and tested till failure. The damaged RC frame structure was retrofitted using GFRP and CFRP and then tested under cyclic loading to explore the effectiveness of FRP's as a strengthening technique. Free vibration test was carried out at every stage of testing such as before testing and after collapse to examine the damage level of the structure. The cyclic behavior of the brick infilled frame before and after retrofitting with both type of FRP's was examined in detail using various parameters such as load carrying capacity, stiffness degradation, energy dissipation and dynamic properties have been considered to evaluate the performance of frames. Dynamic properties were used to define the damage tolerance capacity.

2. Experimental details

2.1 Brick in-filled RC frame

In this study, a one bay three storied building with infill has been designed and scaled down to one third of its actual size for laboratory study. M-20 concrete mix proportions of 1:1.4:2.56 was used to cast the frame with water cement ratio. The cross section of the columns was 100mm reinforced with 4 # 8 mm \emptyset bars and with a floor-to-floor height of 950 mm. All beams were rectangular with a cross section size of 100 mm \times 150 mm reinforced with 2#10 mm \emptyset bars @ top and bottom. All columns and beams were

Table 1 Properties of materials used

Compressive strength of Concrete		
Structural Elements	Compressive Strength (MPa)	Standard Deviation
First floor	24.20	1.48
Second floor	20.84	1.89
Third floor	23.01	1.87
Average	22.46	1.74
Tensile Strength of Steel used		
Steel size	Yield strength (MPa)	Tensile strength (MPa)
Longitudinal bar (10 mm-diameter)	490.18	586.60
Longitudinal bar (8 mm-diameter)	523.43	628.91
Transverse bar (6 mm-diameter)	517.87	636.36
Properties of GFRP and CFRP		
Property	GFRP	CFRP
Tensile strength (GPa)	3.4	4.137
Elastic modulus (GPa)	63	242
Density (g/cm ³)	2.6	1.81

provided with 6 mm diameter stirrups at 100 mm center to center spacing. Throughout the frame, steel grade of Fe500 was used (Fig. 1). Each column was casted integrally with stub foundation, which was in turn bolted firmly with the strong floor and connected with plinth beam of size 150 mm \times 100 mm. Ground storey was designed as soft storey and first and second floor were constructed with brick infills. For mortar preparation, 1:4 cement to sand ratio was used. Top floor was equipped with one Linear Variable Differential Transducer (LVDT) in the horizontal direction. An automated hydraulic actuator was horizontally installed along the desired direction at top floor. Quasi-static loads were applied at uniform rate to simulate structural damage (Fig. 2).

For repair of the damaged frame, two commonly used FRP's namely unidirectional glass fiber reinforced polymer (GFRP) and unidirectional carbon fiber reinforced polymer (CFRP) were used with properties presented in Table 1. The thickness of GFRP sheet used is 0.34 mm whereas the thickness of CFRP sheet used is 1.2 mm. In retrofitting, low viscous epoxy (M Brace Master Injector 1319) was used to fill the internal cracks using injection technique and M Brace putty 2200I was used for surface preparation after



Fig. 3 Control prism



Fig. 4 FRP wrapped prism



Fig. 5 Failed prisms

crack filling. After surface preparation, GFRP sheet was affixed on the damaged portion at each floor and CFRP was used to retrofit the column hinge region in ground floor.

2.2 Performance of FRP and bonding of epoxy with concrete

In order to investigate the vis-a-vis performance of CFRP and GFRP to loads and the effectiveness of the different binders used for bonding property FRP's to concrete, standard prisms of 100×100×500 mm (Fig. 3) were casted. Two control prisms and two samples each repaired with GFRP and CFRP in tension zone were first tested in two point loading (Fig. 4) and tested to failure to estimate the load-deflection characteristics (Fig. 5).

To examine the bonding ability of epoxy in crack filling, further six prisms made of control concrete were tested to failure under two point loading. The broken prisms were reconnected using cement slurry, M Brace 2200 and Master Injector 1315 (M Inj 1315) epoxy (2 samples of each). The reconnected samples were allowed to cure for a week and again tested in two point loading till failure.

From the load deflection behavior of prism specimens tested under two point loading in Fig. 6, it is observed that the FRP strengthened specimens show drastic improvement in the load-deformation characteristics as compared to control prisms. In particular, the specimen repaired at the bottom with higher modulus CFRP possesses better load carrying capacity and the occurrence of crack in un-strengthened part shows the efficiency of the bonding. The

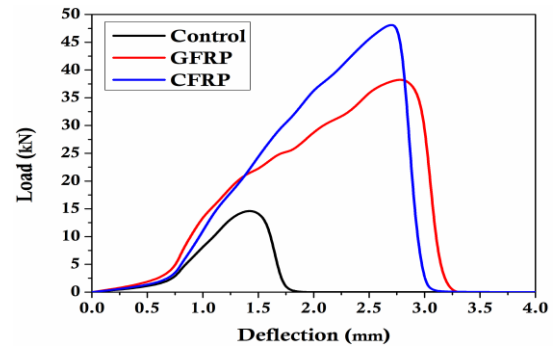


Fig. 6 Load -deflection behaviour of control and FRP repaired prisms

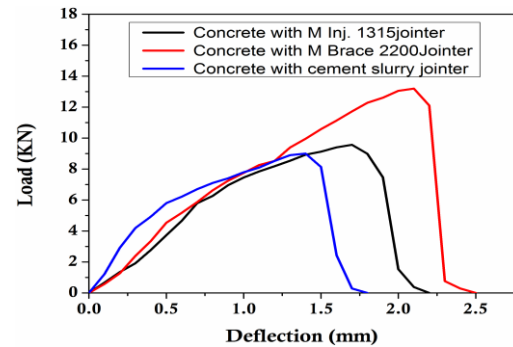


Fig. 7 Flexural strength of reconnected prisms

specimen repaired with GFRP splits into two halves at mid-span and the experiment demonstrates the importance of higher modulus FRP in resisting loads.

The load deflection behaviour of reconnected specimens shows the importance of bonding materials (Fig. 7). The specimen with cement slurry records the least performance over other reconnected specimens. The epoxy enabled specimens show different peak response with respect to the employed epoxy. It proves that the epoxy injection will act as better bonding agent in creating the contact between cracked surfaces. The failure pattern also approves the same trend (Fig. 5). The M Brace 2200 jointer shows the best results and would be further employed for repair of the RC frames.

2.3 Monitoring using impact hammer

Impact hammer test is an important tool to assess the health of a structure without destructing. Each floor of the RC frame was equipped with one accelerometer to measure the vibration in axial loading direction. Impact hammer with a hard rubber tip was used to excite the structure. The signals from the accelerometers were acquired using data acquisition system and Fast Fourier Transform (FFT) spectrum analyzer based software was used to analyze the signal. This vibration measurement predicts the different damage status with respect to the specific frequencies.

2.4 Retrofitting scheme

Initially the RC frame was tested to failure with loading as shown in Fig. 2 and then the deformed frame was

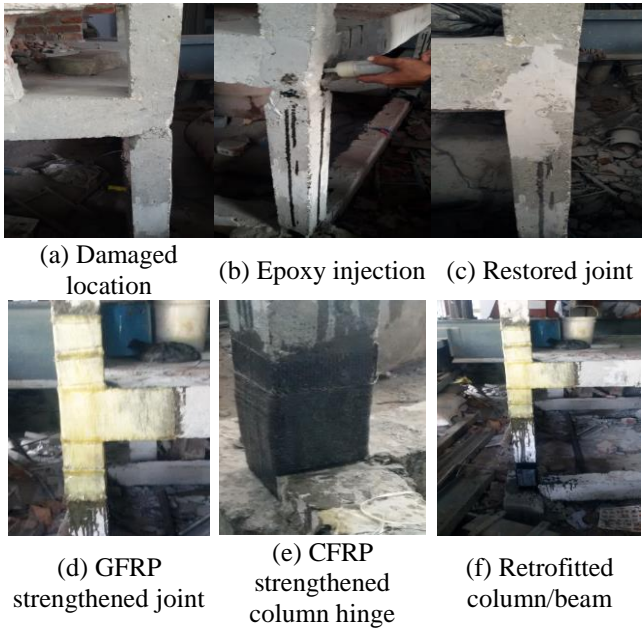


Fig. 8 Strategy for retrofitting of frame

restored again to its initial configuration using a hydraulic system after repairing with FRP strengthening technique. Damaged concrete was removed from the joint region and the surfaces were cleaned of dirt as shown in Fig. 8(a). All the corners of damaged elements were beveled and rounded to a radius of 10 mm in order to avoid corner stress concentration due to sharp edges on FRP. The surface cracks were filled with epoxy as shown in Fig. 8(b) (M Brace 2200 jointer) and then the surface were smoothed. Master injector 1319 was used to fill the internal cracks to create bond between the cracked regions in the damaged part of the frame (Fig. 8(c)). Two different FRP materials such as GFRP and CFRP were used shown in Fig. 8(d). GFRP was used in the beam-column joint of every floors (Fig. 8(e)) and CFRP was used in the strengthening of ground floor hinge location (Fig. 8(f)). FRP sheets had been wrapped in layer by layer wise in two steps: the first layer affixed perpendicular to the loading direction and the second layer was used to confine the existing layer in parallel direction.

3. Results and discussion

3.1 Load-displacement behavior and failure mechanism

The conventional scaled model frame was constructed and tested under quasi-static load. Load was applied by increasing deflection of 5mm in each cycle at the middle of top floor to simulate different level of controlled damage (Fig. 9). The hysteretic behaviour / load - displacement of control and retrofitted frame is shown in Fig. 10. The envelope curve of conventional and retrofitted frame is represented in Fig. 11. The load-displacement envelope curve is used to estimate the lateral deformation capacity (ductility) of the structure at different seismic performance

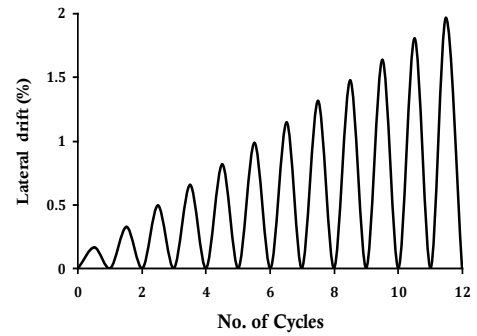
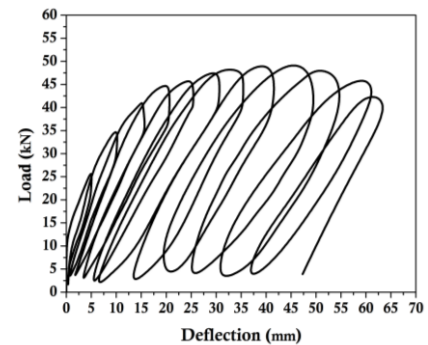
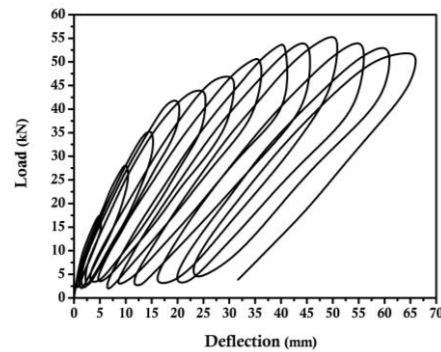


Fig. 9 Loading history



(a) Control frame



(b) Retrofitted frame

Fig. 10 Hysteretic behavior

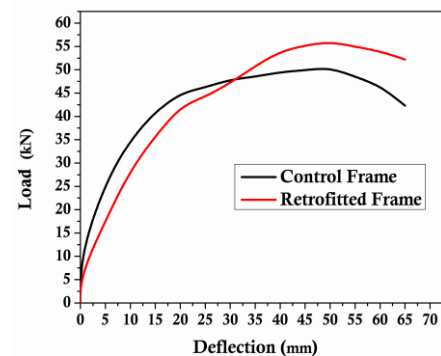


Fig. 11 Envelope curve of conventional and retrofitted frame

levels and the corresponding force modification factor (R) of the structure as per based on FEMA guidelines which are defined as: Linear Limit, Immediate Occupancy (IO), Damage Control (DC), Life Safety (LS), Limited Safety

Table 2 FEMA guidelines for Performance Level and corresponding DI

FEMA Performance Level	A-B	IO	DC	LS	LSR	CP	C
FEMA Damage Index	0	0.17	0.33	0.5	0.67	0.83	1

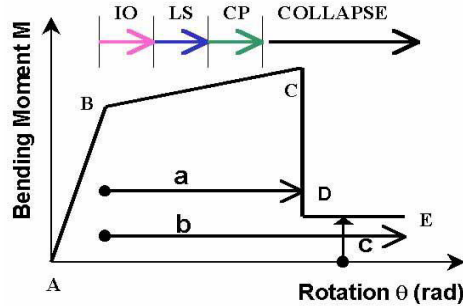


Fig. 12 Failure mechanism of structure as per FEMA guidelines

Structural Range, Collapse Prevention (CP), Collapsed (Table 2, Fig. 12).

The tangential part of the load-deformation curve shows similar almost linear behavior upto yield, followed by non-linear behavior. The hysteretic curves of both frames are distinct in terms of residual deflection. The conventional control RC frame shows higher residual deflection than retrofitted specimen. The retrofitted specimen shows reduced loop area during initial cycles due to the FRP confinement. As a result of the employed yielded reinforcement, the yield deflection is high and yield stiffness is low in retrofitted specimen than control specimens. The retrofitted frame shows 10% higher load carrying capacity and better post yield behavior even with yielded reinforcement. Maximum load was attained at a deflection of 35 mm in conventional and at 45-50 mm in FRP repaired frames showing the confinement resistance offered by FRP to deformation. As the displacement increases, the cracks were formed above and below the strengthened region and hence reduction in load carrying capacity was noticed. But the concrete fails by crushing in the column hinge and joint diagonal cracks shows sudden decrease in load carrying capacity. This shows the structural behavior of both the frames was within LS to CP limits as per ASCE 41-06.

3.2 Energy dissipation

Energy dissipation is estimated by area under the load deformation curve. Fig. 13 shows the energy dissipation curve of the control and retrofitted frames. The performances of both the frames are similar upto a deflection of 45 mm. As a result of severe cracking in the hinge region, the conventional frame failed to show better post peak load carrying capacity and a decrease in the energy dissipation capacity after 45 mm is noticed in the conventional control frame. On the other hand, in the retrofitted frame, no sudden failure is observed and better post peak performance is seen. The retrofitted frame shows

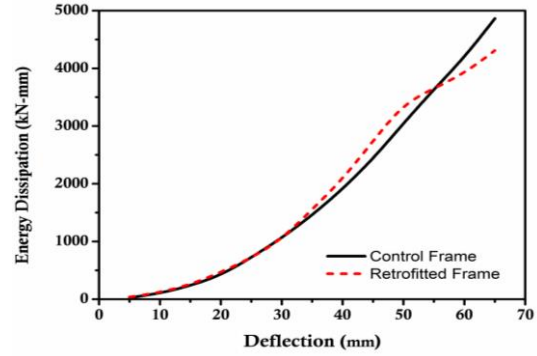


Fig. 13 Energy dissipation V/s deflection of control and retrofitted frame

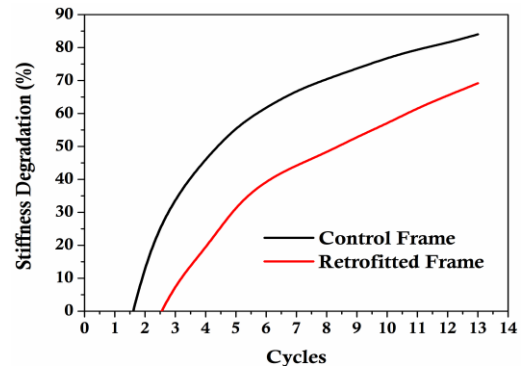


Fig. 14 Stiffness degradation in control and retrofitted frame

gradual and increased energy dissipation capacity as compared to the control frame.

3.3 Stiffness degradation

The difference between the initial and secant stiffness shows the post yield behavior of a structural component. In this study, the degradation in stiffness is calculated in terms of post elastic stiffness degradation over yield stiffness [represented by $K_{deg}\%$] using the Eq. (1). The rate of change of stiffness degradation over the post elastic range is the measure of inelastic performance of the component.

$$K_{deg}\% = \left[1 - \frac{(K - K_y)}{K_y} \right] * 100 \quad (1)$$

Where: K - Stiffness of each cycle, kN/mm; K_y - Yield stiffness, kN/mm

Sudden or rapid degradation in stiffness shows the brittle performance while low rate of stiffness degradation shows ductile performance. The comparative curve of both the specimens shows that the loss of yield stiffness is high in retrofitted specimens than conventional. This is because of the employed yielded reinforcement in the RC frame. In the damaged RC frame, the surface concrete in the impaired location has been thoroughly removed and replaced with epoxy putty and the internal cracks were injected with epoxy. But the reinforcement in the hinge region was not replaced and hence all the hinge regions were critically strengthened using external FRP reinforcement. Thus, the



Fig. 15 Damage in column-beam and column-foundation after loading in control frame

retrofitted specimens show higher loss in initial and yield stiffness than conventional frame. But the post elastic stiffness degradation is comparatively low in retrofitted frame as compared to control frame. It illustrates the influence of external FRP strengthening in non-linear performance. The stiffness degradation versus post elastic drift for each tested frame specimen is plotted in Fig. 14.

3.4 Crack pattern

The crack pattern was critically monitored and marked on the surface of the specimen during the testing. Four columns were marked as A, B, C, D for identification as shown in Fig. 15(a). The brick infill in the first and second storey made the ground storey soft and hence the failure intensity was high in the ground storey. The plastic hinge formation was noticed exactly below the first floor beam-column joint connection and at the column foundation connection. Initially flexural cracks were noticed at the beam-column connection region followed by joint shear cracks. As the deformation increased, dense cracks were noticed at the foundation hinge region as depicted in Fig. 15 (b)-(i). Predominant cracking was observed in the first floor

beam-column joint region whereas the second and roof have no evidence of cracking because of the soft storey effect. The witnessed horizontal crack below the joint region reduced the stiffness and restricted the deformation capacity even though followed by shear cracks in the joint region. As a result of the dense crack concrete cover spalling was occurred in the joint region. The effect of seismic detailing supports the RC frame to deform but the brittle nature of concrete exhibits concrete crushing failure at the foundation hinge region. There is no severe damage in the infill; horizontal sliding cracks were noticed in the infill at the mortar joints as shows in Fig. 15(i).

In retrofitted frame, the internal cracks were injected with epoxy and after a thorough surface preparation, FRP wrapping was done. Thus, the failure pattern of the retrofitted frame is different from control frame. The FRP strengthening at the column hinge location and beam-column joint made strengthened portion stiffer and hence failure was concentrated in the unstrengthened region. Fig. 16(a)-(h) shows the cracks below and above the strengthened portion followed by FRP rupture in few locations. The primary failure is because of the horizontal crack below the FRP strengthened region. Thus the ultimate

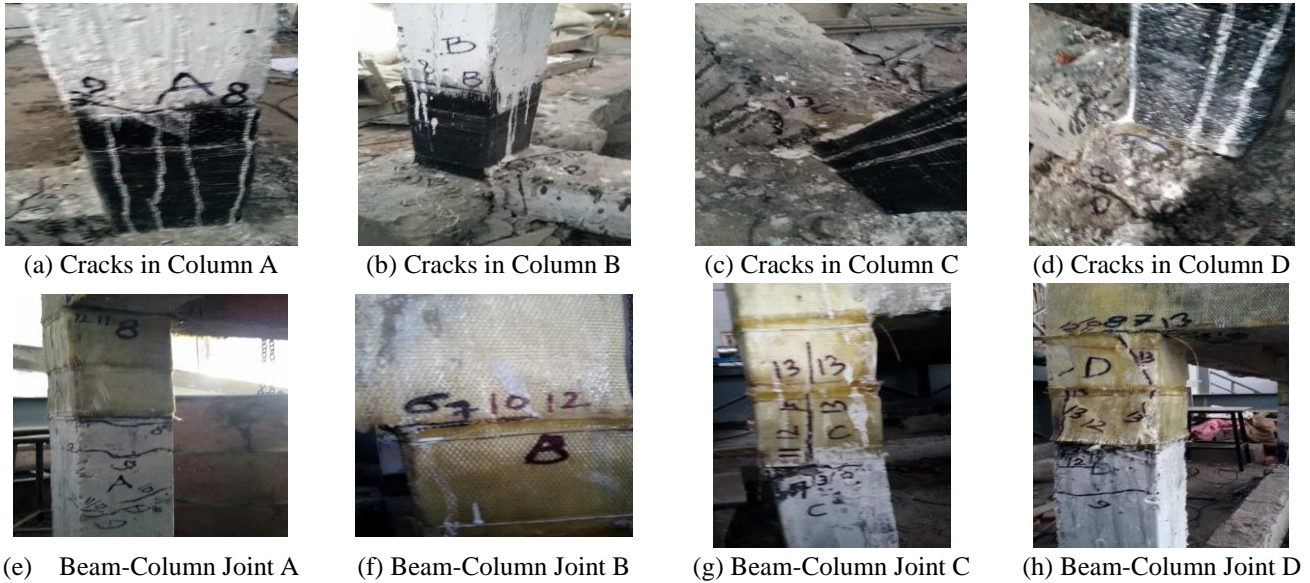


Fig. 16 Damage in Column-Beam and Column-Foundation after loading in retrofitted frame

deformation of the strengthened frame is identical with the control frame.

3.5 Damage Index based on dynamic characteristics

The damage tolerance capacity of the frames has been estimated using the Damage Index (DI) (Kanwar *et al.* 2010), Eq. (2). which uses an indicator based on the relationship between the material stiffness properties of the undamaged element and the damaged element of the structure. According to this method severity of damage is expressed as the fractional change in stiffness of an element:

$$DI_k = \frac{k_j - k_j^*}{k_j} = 1 - \frac{1}{v_j} \quad (2)$$

Where, v_j is stiffness ratio, k_j is initial stiffness of undamaged element and k_j^* is the initial stiffness of the damaged element of the j^{th} member. The asterisk (*) denotes the damage state.

It shows that as the load increases in every cycle the damage increases. The brittle nature of concrete allows early crack formation in the hinge region. Thus the damage index plot shows early damage in control frame over retrofitted. The presence of FRP in the plastic hinge region of beam and column resist the load effectively without any crack in the joint. The cracks were initiated above and below the FRP strengthened region. The effective confinement of FRP allows the frame deforms and restricts early joint failure. Thus its shows 0.4 DI at 10th cycle where as it is 0.55 for control frame. The DI of retrofitted frame shows sudden increase after 10th cycle. This is possibly because of the occurrence of severe damage in the unconfined region and part of FRP rupture during larger deformation.

3.6 Dynamic characteristics

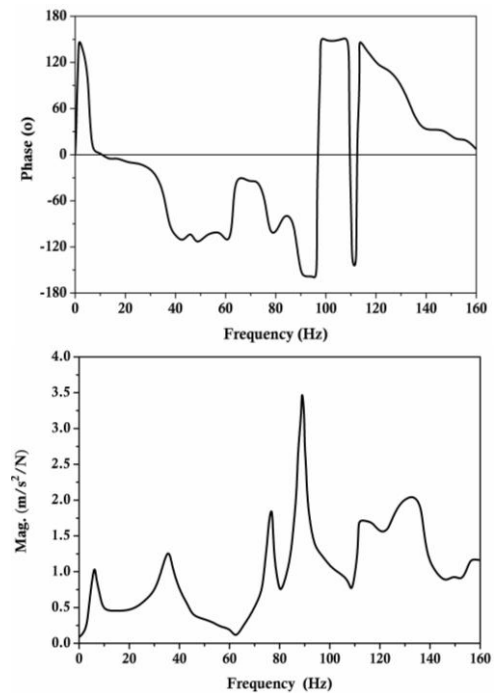


Fig. 17 Frequency response function

Table 3 Frequency and damage index of control and retrofitted frame

Damage	Conventional Frame		Retrofitted frame	
	Frequency	Damage index	Frequency	Damage index
0 Damage	7	0	7.6	0
After 2 nd Cycle	6.9	0.063	7.2	0.057
After 4 th Cycle	6.7	0.162	7.0	0.138
After 6 th Cycle	6.4	0.309	6.7	0.201
After 8 th Cycle	5.9	0.476	6.0	0.360
After 10 th Cycle	5.2	0.655	5.4	0.521
After 13 th Cycle	4.8	0.832	4.8	0.786

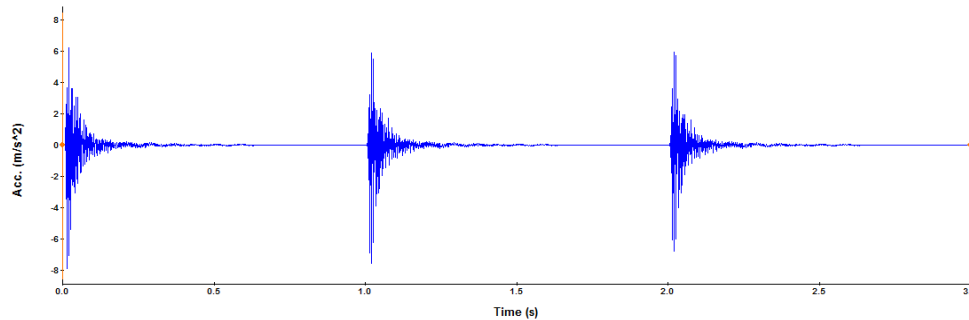


Fig. 18 Time history plot

The dynamic characteristics of a structural system can be estimated from the frequency response function (FRF) shown in Fig. 17 and Time History plot shown in Fig. 18. The FRF based damage index is one of the most effective ways in health monitoring. The change in fundamental frequency and magnitude of FRF of a system defines the damage behaviour. In this study, an impact hammer and accelerometer were used to acquire the FRF and the logarithmic decrement defines the equivalent damping response. The usual aim of vibration measurement is to predict response given force in different damage status. The specific frequencies at which resonance amplitudes occur are called the natural frequencies of the structure. These frequencies and the corresponding distribution of amplitude are global properties. The calculated frequency and damage index are presented in Table 3.

The conventional and retrofitted frame shows similar kind of frequency response. The test results show a reduction in the natural frequency as the damage level increases. The conventional specimens show natural frequency ranging from 7-4.8 Hz with the change in damage index 0 to 0.669. The natural frequency reduces as the damage level increases; thus, it shows a 31.4% reduction in natural frequency at failure stage. The FRF magnitude is found to decrease and damping ratio is found to increase with the increase in deformation. Thus, the conventional frame shows a 66.9% reduction in FRF magnitude and a 64% increase in damping ratio.

The retrofitted frame specimen shows a similar trend to conventional frame frequency response. The observed natural frequency of conventional specimen varies from 7.6 to 4.8 Hz with the change in damage index 0 to 0.662. It shows a 36.8% reduction in natural frequency at failure stage. This proves the effectiveness of the strengthening technique adopted in restoring the frame. There was a tremendous change in FRF magnitude and damping ratio, showing remarkable energy dissipation capacity of the retrofitted frame as compared to conventional frame. The observed FRF reduction of the retrofitted frame is 66.2% and 72% increase in damping ratio.

4. Conclusions

This experimental study mainly focuses on investigation of control and retrofitted RC frame under cyclic loading. The hysteretic curve, stiffness retention, energy dissipation,

damage tolerance and failure pattern are the main parameters used in this study to examine the efficiency. Major conclusions derived from the study can be summarized as below:

1. There is a significant improvement in the load carrying capacity of FRP strengthened and epoxy injected reconnected prisms under two-point bending. It was observed that the reconnected point sustained and further the crack was found below the load point. It proves the effectiveness of epoxy in bonding.
2. Hysteresis behavior of the FRP repaired RC frame shows better post yield behavior and enlarged loop area under cyclic loading. Also, the residual deflection is lesser in FRP strengthened than the control specimen due to better damage tolerance. It shows that the FRP strengthened frame offers better elastic and inelastic behavior.
3. The employed existing yielded reinforcement in FRP repaired frame failed to show better initial and yield stiffness than the control specimen. Even though, with lesser initial stiffness, the retrofitted frame provides better post yield stiffness retention as compared to control specimen. This kind of retrofitting and FRP strengthening may be an effective method in restoring the structural integrity.
4. The enlarged loop area shows better dissipated energy level and damage tolerance capacity of adopted strengthening technique in the retrofitted frame. The dynamic test also proves the same trend in damage tolerance. The crack pattern and failure behavior shows that the strengthened portion is more sustainable than the un-strengthened region. The failure area is mainly concentrated in the weakest portion of the frame, but FRP strengthening in the hinge region supports the frame to provide better inelastic deformation.

References

- Ceroni, F. (2010), "Experimental performances of RC beams strengthened with FRP materials", *Constr. Build. Mater.*, **24**(9), 1547-1559.
- Kakaletsis, D.J. (2016), "Comparative experimental assessment of seismic rehabilitation with CFRP strips and sheets on RC frames", *Eartq. Struct.*, **10**(3), 613-628.
- Kanwar, V., Kwatra, N. and Aggarwal, P. (2007), "Damage detection for framed RC buildings using ANN modelling", *J.*

- Damage. Mech.*, **16** (4), 457-472.
- Kanwar, V., Kwatra, N., Aggarwal, P. and Gambir, M.L. (2006), "Vibration monitoring of A RC building model", *Proceedings of the National Conference on Technology for Disaster Mitigation*, Hamirpur, India.
- Kanwar, V., Kwatra, S., Aggarwa, N., Singh, S. and Ramesh, P. (2010) "Use of vibration measurements in health monitoring of reinforced concrete buildings", *Int. J. Struct. Integrity*, **1**(3), 209-232.
- Kanwar, V., Singh, S., Ramesh, P., Kwatra, N. and Aggarwal, P. (2016), "Monitoring of RC structures affected by earthquakes", *Geomat. Nat. Hazard. Risk*, **7**(1), 37-64.
- Lakshmikandhan, K.N., Sivakumar, P. and Ravichandran, R. (2012), "Cyclic load performance evaluation of reinforced concrete beam and repaired concrete beam", SERC Research Report No. CAD/OLP 14441/RR- (15).
- Lakshmikandhan, K.N., Sivakumar, P. and Ravichandran, R. (2013), "Damage assessment and strengthening of reinforced concrete beams", *Int. J. Mater. Mech. Eng.*, **2**(2), 34-42.
- Mukherjee, A. and Joshi, M. (2005), "FRP reinforced concrete beam-column joints under cyclic excitation", *Compos. Struct.*, **70**, 185-199.
- Mukherjee, A., Boothby, T.E., Bakis, C.E., Joshi, M.V. and Maitra, S.R. (2004), "Mechanical behavior of fiber reinforced polymer wrapped concrete columns-complicating effects", *J. Compos. Constr.*, **8**(2), 97-103.
- Noman, A.S., Deebea, F. and Bagchi, A. (2009), "Structural Health Monitoring using vibration-based methods and statistical pattern recognition Techniques", *Proceedings of International Workshop on Smart Materials and Structures*, Montreal, Quebec, October.
- Omar, A. and Stefan, K. (2014), "Modelling of circular concrete columns with CFRP sheets under monotonic loads by ATENA-3D", *Forecast Engineering: Global Climate Change and the Challenge for Built Environment*, 1-15.
- Onur, T. and Ozgur, A. (2017), "Seismic repair of captive-column damage with CFRP in substandard RC frames", *Struct. Eng. Mech.*, **61**(1), 1-13.
- Ooijsavaar, T. H., Loendersloot, R., Warnet, L. L., de Boer, A. and Akkerman, R. (2010), "Vibration based Structural Health Monitoring of a composite T-beam", *Compos. Struct.*, **92**, 2007-2015.
- Ozgur, Y. and Ozgur, A. (2015), "Structural repairing of damaged reinforced concrete beam- column assemblies with CFRPs", *Structl. Eng. Mech.*, **54**(3), 521-543.
- Park, Y.J. and Ang, A.H.S. (1985), "Seismic damage analysis of RC buildings", *ASCE J. Struct. Eng.*, **111**(4), 740-757.
- Said, A.M. (2009), "Damage characterization of beam-column joints reinforced with GFRP under reversed cyclic loading", *Smart Struct. Syst.*, **5**(4), 443-455.
- Sathiaseelan, P. and Arulselvan, S. (2015), "Influence of Ferrocement retrofit in the stiffened in the fill RC frame", *Int. J. Sci. Tech.*, **8**(30), 1-6.
- Shraideh, M.S. and Aboutaha, R.S. (2013), "Analysis of steel-GFRP reinforced concrete circular columns", *Comput. Concrete*, **11**(4), 351-364.
- Vimuttasoongviriyaya, A., Kwatra, N. and Kumar, M. (2009), "Effect of lateral quasi-static load on nonlinear behaviour and damage indexes of retrofitted RC frame model", *Asian J. Civil Eng.*, **10**(5), 563-588.
- Vimuttasoongviriyaya, A., Kwatra, N. and Kumar, M. (2010), "Damage detection of strengthened RC frame model with FRP sheets under lateral loads", *Proceedings of 11th International Conference on Structures under Shock and Impact*, Estonia.
- Vimuttasoongviriyaya, A., Kwatra, N. and Kumar, M. (2010), "Modal parameters damage method for detecting damage in strengthened RC frame model using GFRP laminate", *Proceedings of 15th National Conference in Civil Engineering*, Ubonratchathani, Thailand.
- Vimuttasoongviriyaya, A., Kwatra, N. and Kumar, M. (2010), "Nonlinear behaviour and vibration based damage identification of retrofitted RC frame model", *Proceedings of 9th International Conference for High Rise Towers and Tall Buildings*, Munich, Germany, Paper ID 0958.
- Vimuttasoongviriyaya, A., Kwatra, N. and Kumar, M. (2011), "Vibration monitoring and damage assessment of a retrofitted RC frame model", *KMITL Sci. Tech. J.*, **11**, 43-53.
- Wang, K., Inman, D.J. and Farrar, C.R. (2005), "Modelling and analysis of a cracked composite cantilever beam vibrating in coupled bending and torsion", *J. Sound Vib.*, **284**, 23-49.
- Xu, B., Song, G. and Masri Sami, F. (2012), "Damage detection for a frame structure model using vibration displacement measurement", *Struct. Hlth. Monit.*, **11**(3), 281-292.

CC